Detection and Mitigation of Strong Azimuth Ambiguities in High Resolution SAR Images

Rolf Scheiber, German Aerospace Center (DLR), rolf.scheiber@dlr.de, Germany
Marc Jäger, German Aerospace Center (DLR), marc.jaeger@dlr.de, Germany

Abstract

Azimuth ambiguities of bright point-like targets become more pronounced in case of high resolution SAR imaging. When improving the spatial resolution, the compression gain in SAR image formation becomes larger, which increases the dynamic range of SAR images. The increased point target intensity also implies a correspondingly higher azimuth ambiguity power, which often exceeds the reflectivity of the surrounding homogeneous areas. This paper proposes a new approach to identifying and mitigating azimuth ambiguities of bright targets within areas of distributed homogeneous backscattering. The method makes use of two independent range looks. While the main signal in the two looks is considered nearly identical, the ambiguous signal becomes mis-registered, i.e. the azimuth position shifts as a function of the range look center frequency. This property is used to derive a suitable mitigation approach. It is tested with X-band data acquired by DLR's F-SAR sensor in step-frequency mode.

1 Introduction

The origin and characteristics of azimuth ambiguities in SAR images are well understood [1]. The most efficient way to suppress ambiguities is by proper design of the SAR antenna pattern. Doing so is, however, a trade-off between data rate, available transmit power and the desired resolution [2]. Antennas that are not tapered in azimuth are particularly problematic, as the azimuth level is at approx. 25dB below the main lobe, as determined by the sidelobes of the antenna pattern. In case of PRF constraints, even part of the main-lobe might contribute to ambiguous energies. Different ways of estimating the ambiguity ratio and correcting the data have been proposed in the past. In part they assume that the primary target is within the scene [3]. Alternatives propose the use of a Wiener filter making use of the different spectral shape of ambiguities and main signal [4]. This paper presents a different approach. It makes use of two range looks, thus exploiting the ambiguity location dependence on wavelength.

2 Theoretical background

2.1 Azimuth location of ambiguities

The relative mis-location of azimuth ambiguities from the primary signal can easily be derived from the exact time-Doppler relationship and is given by:

$$\Delta_{az} = \frac{\lambda(f_r)PRF}{2v\sqrt{1-(\frac{\lambda(f_r)PRF}{2v})^2}}\frac{h}{\cos\theta}, \quad (1)$$

where PRF is the radar's pulse repetition frequency, v is platform forward velocity, h is altitude of the platform and θ is the incidence angle. Most important in the context of high resolution SAR is a dependency on the wavelength λ, which varies within the bounds of the transmit pulse bandwidth ($f_c - B/2 \leq f_r \leq f_c + B/2$). This variation is responsible for the azimuth spread of the ambiguous signal. For large system bandwidth, this spread can become much larger than the azimuth resolution. The mis-location according to eq. 1 is evaluated in Figure 1 for the case of the airborne SAR parameters listed in Table 1, corresponding to the F-SAR system of DLR [5].

Parameter	Value
center frequency	9.6 GHz
pulse bandwidth	100 - 1000 MHz
3dB antenna width	8 deg
PRF	1000 Hz
platform velocity	90 m/s
flight altitude	3000 m
incidence angle	25 - 65 deg

Table 1: Airborne SAR sensor parameters.

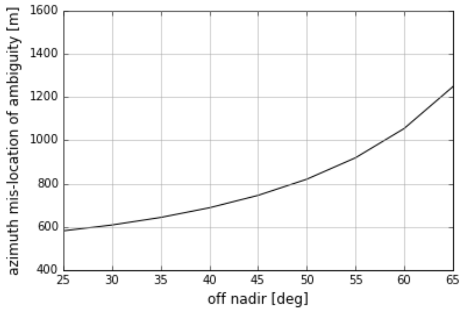

Figure 1: Azimuth displacement of the ambiguity from the main signal for the airborne geometry of Table 1.

There is also a mis-location and spread of ambiguous energy in the range direction due to the wrongly compen-

ISBN 978-3-8007-4228-8 / ISSN 2197-4403

sated range cell migration. This effect causes additional defocussing in azimuth but is irrelevant to the present approach.

2.2 Azimuth ambiguities for different range looks

Because of the wavelength dependence, the azimuth ambiguities of a bright target are not co-located in different range looks. The total spread of ambiguous energy in the full-resolution image, assuming the system parameters of Table 1, is evaulated in 2. The azimuth separation between two half-band range looks corresponds to half of the indicated spread. Since the ambiguities' relative mislocation is much larger than the resolution of the SAR sensor, suitable methods can be found to detect and mitigate them. This will be discussed in the following section.

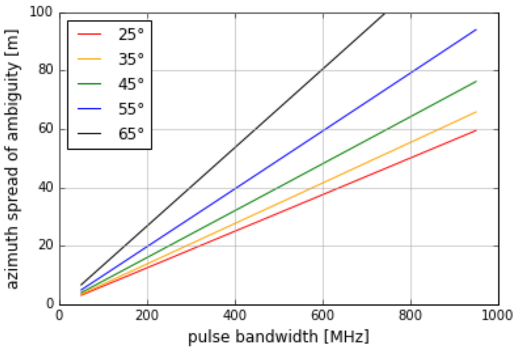

Figure 2: Azimuth spread of ambiguous signals as a function of signal bandwidth. The airborne geometry of Table 1 is considered.

3 Ambiguity mitigation

The algorithm for detecting and mitigating the ambiguities is summarized in the block diagram of Figure 3. Two range-looks are computed from the lower and upper half-band spectrum, respectively, followed by multi-looking for reduction of Speckle. The detection of ambiguous image areas is then performed by contrasting the two Speckle-filtered range look images (orange). This works well for most of the ambiguities' spread, except for the central azimuth position of each ambiguity, where the ambiguous signal is nearly co-located in the two looks. As described in more detail in section 3.1, these positions can be detected by inspecting the ambiguity mask. The ambiguity removal step then replaces the high resolution image content by the respective half-band filtered images unaffected by ambiguity spread (blue). For the the central position a quarter-bandwidth filtered image is used (green). Details of the algorithm steps are described in the following. Figure 4 shows the fully polarimetric F-SAR data set used to validate the approach. It is taken from an X-band step-frequency acquisition with 760 MHz bandwidth that was processed to an azimuth resolution of 0.25 m.

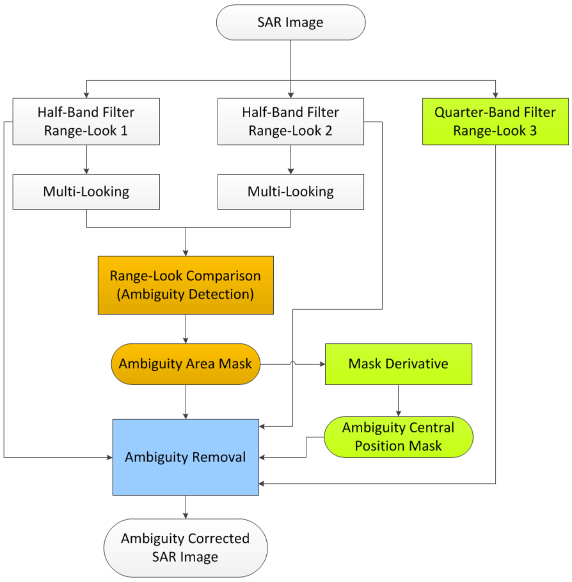

Figure 3: Data flow for the proposed ambiguity detection and mitigation approach.

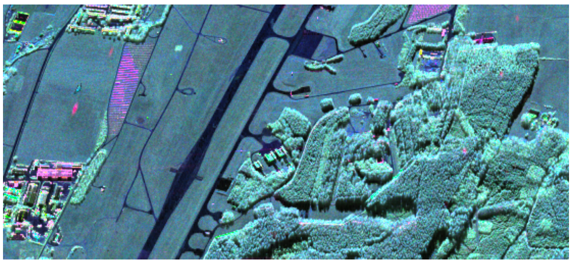

Figure 4: Sub-set of a polarimetric F-SAR scene in Pauli basis (R:HH-VV, G:HV+VH, B:HH+VV). The bright red spots in the image are azimuth ambiguities of large trihedral reflectors and the green one most likely is a moving target. Flight direction is horizontal and illumination is from top.

3.1 Detection of ambiguities

Several details need to be considered to ensure the reliable detection of the complete spread area of the ambiguities. It is recommmended to generate the range looks without any weighting of the band-filtered range spectrum. This will enlarge the areas affected by noticeable ambiguous energy, which eases their detection. The size of the multilook window should be comparable to the extent of the ambiguous area (approx. 100 x 100 samples). According to eq.(1), the areas affected by the upper and lower bandwidth ambiguities are complementary and their size is half of the ambiguous area of the full resolution image (see Figure 5 (top)). However, depending on the chosen threshold for contrasting the two filtered range-look images, the central ambiguity area will not be detected properly since the filtered range look images will present very similar ambiguous energy as a result of the

ISBN 978-3-8007-4228-8 / ISSN 2197-4403

resolution loss due to multi-looking. Thus there is a need for a second, so called central ambiguity mask. Luckily, these areas can be easily identified from the specific signature in the ambiguity mask detected before. We implemented a simple energy balancing method, in which the ambiguity mask is correlated with a step-function line by line. The size of the steps (adjacent but with opposite sign) is half the ambiguities' spread (see Figure 2). This precisely marks the location of the ambiguities' center positions, which can then be enlarged to produce the mask shown in Figure 5 (bottom). A sketch showing the individual steps for generating the two masks is presented in Figure 6.

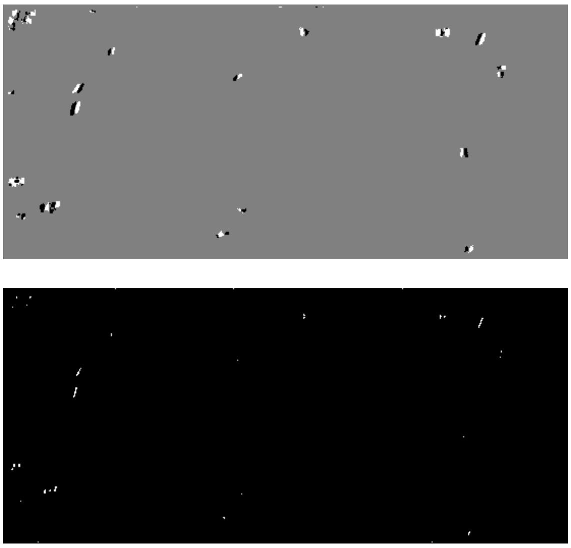

Figure 5: Detected ambiguity areas using two range looks (top) and central ambiguity area for quarter bandwidth filtering (bottom). These are the masks derived on the basis of the example dataset in Figure 4.

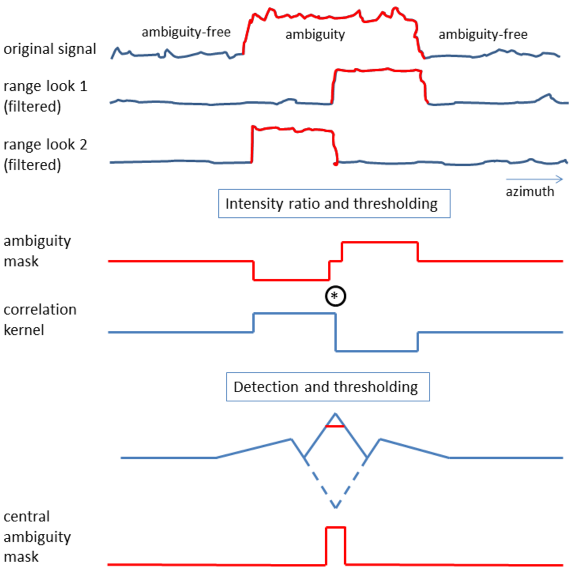

Figure 6: Sketch showing the detection of the two ambiguity masks.

3.2 Compensation of ambiguities

The compensation of ambiguous areas corresponds to simply replacing the areas identified in the two masks by either one of the two half-band (ambiguity mask) or by the quarter-band filtered complex data. In these very localized regions the range resolution will thus be reduced by a factor of 2 or 4. Since multi-looking will usually be performed for any subsequent evaluation, this will correspond to a localized reduction of the effective number of looks. The ambiguity corrected SAR image is presented in Figure 7.

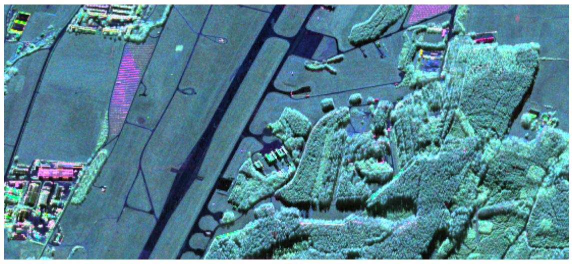

Figure 7: Sub-set of the polarimetric F-SAR scene of Figure 4) after compensation of ambiguities using the proposed approach.

3.3 Considerations for Interferometric and Polarimetric Data

In order to avoid coherence degradation due to potentially different ambiguity masks in master and slave interferometric pairs, it is suggested to apply the ambiguity detection on the master image only and then apply the removal in an identical way to the master and co-registered slave. A slight mis-registration of ambiguities in master and slave images, which might occur for larger baselines, will not influence the performance in a noticeable way due to the strong multi-looking performed during ambiguity detection.
As ambiguities are often caused by man-made structures, they are usually associated with a particular polarimetric signature. For polarimetric data, it is therefore suggested to apply the first step of the ambiguity detection process independently for each polarisation, before using their logical disjunction as a combined mask for all polarisations (see Figure 5). In this way the polarimetric signature of the underlying main signal is not distorted by potentially different range resolutions in the different polarisations.
In the context of SAR polarimetry, it is also important to recall the ambiguity analysis of Freeman [6], suggesting that the two cross-polarised channels (HV and VH) might not only be used for noise estimation, but also for the detection and even removal of cross-pol ambiguities. This is because azimuth ambiguities in HV and VH channels are usually 180 deg out of phase due to the PRF-toggled data acquisition strategy, whereas areas free of ambiguity ideally show a zero degrees HV-VH phase. The same 180 deg effect also applies for the HH-VV phase difference

ISBN 978-3-8007-4228-8 / ISSN 2197-4403

of first order ambiguities, which for our example leads to the red color of the ambiguous areas in Figure 4, suggesting double- or even-bounce scattering, whereas the originating main signal is odd-bounce (trihedral reflector). Thus, although fully polarimetric data can be used to detect cross-polar ambiguities, they cannot be used for reliable detection of the co-polar ones, a limitation that the approach suggested in this paper can overcome. For comparison Figure 8 displays the areas affected by cross-polar ambiguities as detected from the cross-polar phase difference. In part the detections are coincident with those for the suggested approach (see Figure 5), however the majority is related to low backscatter areas (e.g. runway) and shadow, characterized by low signal-to-ambiguity ratios.

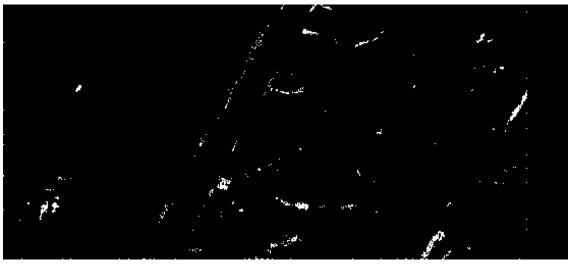

Figure 8: Detected ambiguity areas using the cross-polar phase, for the example data set in Figure 4.

4 Applicability to Spaceborne Data

The applicability of the suggested algorithm strongly depends on the ratio of azimuth resolution and spread of ambiguous energy. This ratio is approximately 0.004 for the example airborne F-SAR case (azimuth resolution of 25 cm vs. 60 m spread).

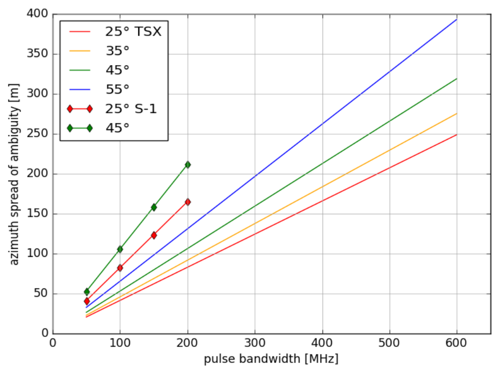

Figure 9: Azimuth spread of ambiguous signals as a function of signal bandwidth for the spaceborne case. The TerraSAR-X and Sentinel-1 cases are considered and extrapolated to higher bandwidths.

For comparison, the spread for the present spaceborne sensors TerraSAR-X and Sentinel-1 is quantified in Figure 9 showing slightly larger values as in the airborne case. However, taking into account the stripmap azimuth resolutions of TerraSAR-X (3m) and Sentinel-1 (5m) the ratio becomes approximately 0.04 for TSX and 0.1 for S-1. In addition, the compression gain for point-like targets in spaceborne SAR data is at least 16dB lower than in the discussed airborne case. Thus present day spaceborne data are therefore less susceptible to the the type of ambiguities discussed in this paper. However, in case of the Staring-Spotlight TerraSAR-X data (300 MHz bandwidth and 0.25 m azimuth resolution), the ratio becomes comparable to the airborne case and the suggested approach may be useful in improving data quality.

5 Final Discussion

The ambiguity detection and mitigation approach proposed in this paper applies primarily to high resolution data. It is capable of identifying isolated azimuth ambiguities with intensities coniderably above the co-located main signal. The approach is likely to fail or perform less well when the size of the high reflectivity objects of the main signal causing the ambiguity becomes comparable to the azimuth spread of ambiguous energy. In these cases the ambiguous areas in the two-range looks are not completely separable, thus ambiguities remain undetected and cannot be removed. It was shown that the method applies well to sub-meter resolution airborne data, whereas it is probably not suitable for present day spaceborne sensors. However, it might become a useful approach for improving image quality for future higher resolution SAR sensors. In general, however, it should be noted that eliminating ambiguities at the antenna design stage should always be the preferred solution.

References

[1] J.C Curlander and R.N. McDonough: *Synthetic Aperture Radar Systems and Signal Processing*, John Wiley & Sons, New York, pp. 296ff, 1988.

[2] A. Freeman, et al: *The 'myth' of the minimum SAR antenna area constraint* , IEEE Transactions on Geoscience and Remote Sensing, vol. 38,no. 1, pp. 320-324, 2000.

[3] A. Monti Guarnieri: *Adaptive removal of azimuth ambiguities in SAR images*, IEEE Transactions on Geoscience and Remote Sensing, vol. 43,no. 3, pp. 625-633, 2005.

[4] M. Villano and G. Krieger: *Spectral-Based Estimation of the Local Azimuth Ambiguity-to-Signal Ratio in SAR Images*, IEEE Transactions on Geoscience and Remote Sensing, vol. 52,no. 5, pp. 2304–2313, 2014.

[5] A. Reigber, et al: *Very-High-Resolution Airborne Synthetic Aperture Radar Imaging: Signal Processing and Applications*, IEEE Proceedings, vol. 101, no. 3, pp. 759-783, 2013.

[6] A. Freeman: *The effects of noise on polarimetric SAR data*, IEEE International Symposium on Geoscience and Remote Sensing, Tokyo, Japan, 1993.